

Enhanced device performance of organic solar cells *via* reduction of the crystallinity in the donor polymer†

Jong Hwan Park,^a Jeong-Il Park,^b Do Hwan Kim,^b Joo-Hyun Kim,^a Jong Soo Kim,^a Ji Hwang Lee,^a Myungsun Sim,^a Sang Yoon Lee^b and Kilwon Cho^{*a}

Received 11th March 2010, Accepted 15th April 2010

First published as an Advance Article on the web 10th June 2010

DOI: 10.1039/c0jm00664e

A new π -conjugated polymer, poly(2,5-dioctyloxyphenylene vinylene-alt-3,3-dioctylquater thiophene) (PPVQT-C8), consisting of alternating p-divinylene phenylene and 3,3-dialkylquater thiophene units, was synthesized for use in organic solar cell devices. The crystallinity of poly(quaterthiophenes) (PQTs) was reduced by introducing p-divinylene phenylene units between pairs of quaterthiophene units. A well-mixed nanoscale morphology of PPVQT-C8:PCBM photoactive layer resulted from this modification, which increased the power conversion efficiency relative to devices based on highly crystalline PQTs. Bulk heterojunction solar cells based on PPVQT-C8:PC₆₀BM blends with a 1 : 3 ratio presented the best photovoltaic performances, with a short-circuit current density (J_{sc}) of 6.7 mA cm⁻², an open-circuit voltage (V_{oc}) of 0.67 V, a fill factor (FF) of 0.62 and a power conversion efficiency (PCE) of 2.8% under illumination of AM 1.5 with light intensity of 100 mW cm⁻². The charge carrier mobility and morphology studies indicated that an optimized interpenetration network composed of PPVQT-C8:PCBM could be achieved in a blend ratio of 1 : 3.

1. Introduction

The development of highly efficient electron donor and acceptors materials is a key issue in developing high efficiency organic bulk heterojunction solar cells.^{1–6} For efficient light absorption, donor and acceptor materials should have a high absorption coefficient and a low optical band gap.⁷ High carrier mobilities are also needed to minimize recombination and trapping of charge carriers during transport to the electrodes. Donor and acceptor molecules must be well-mixed in bulk heterojunctions on the length scale of 10–20 nm in each domain because exciton recombination significantly increases when the domain sizes of the donor or acceptor materials exceed the exciton diffusion length.^{8,9} Crystalline organic semiconductors show higher carrier mobilities^{10–13} than amorphous organic semiconductors because the strong π – π interactions enable fast in-plane charge transport. However, the photovoltaic properties of conjugated polymers with higher carrier mobilities are not always good due to macrophase separation of the active layers during post-fabrication treatment process.^{12–15} Furthermore, the performances of solar cell devices based on highly crystalline materials depend strongly on the processing conditions, such as the residual solvents,¹⁶ additives,¹⁷ and post-fabrication treatment methods,^{18,19} which increase the complexity of device processing.

Poly(quater thiophenes) (PQTs) are promising candidates for high efficiency organic solar cells due to good light absorption

properties and a high hole mobility.¹⁰ However, the photovoltaic performances of PQT and PC₆₀BM-based devices are very poor (<1%).^{14,15} Even if PQT:PC₆₀BM-based devices are thermally treated under mild conditions (~50 °C), macrophase separation of the active layers, which results in low photocurrent and a poor FF, occurs due to the PQTs' high crystallinity.¹⁴ In this paper, we describe a new p-type conjugated copolymer (PPVQT-C8) composed of alternating p-divinylene phenylene and 3,3-dialkylquaterthiophene units for use in organic solar cell applications. To minimize the complexity of device processing and to maintain good mixing of the donor and acceptor materials in the bulk heterojunction photoactive layers during operation, we reduced the crystallinity of PQTs by introducing p-divinylene phenylene units between each pair of quaterthiophene units. Bulk heterojunction solar cells based on the PPVQT-C8:PC₆₀BM blend were fabricated, and their performances were optimized. The nanophase separation of copolymer:PCBM blend layers was found to be correlated with reduced crystallinity in the copolymer. The dependence of solar cell performance on composition ratio and thermal treatment was systematically studied.

2. Experimental

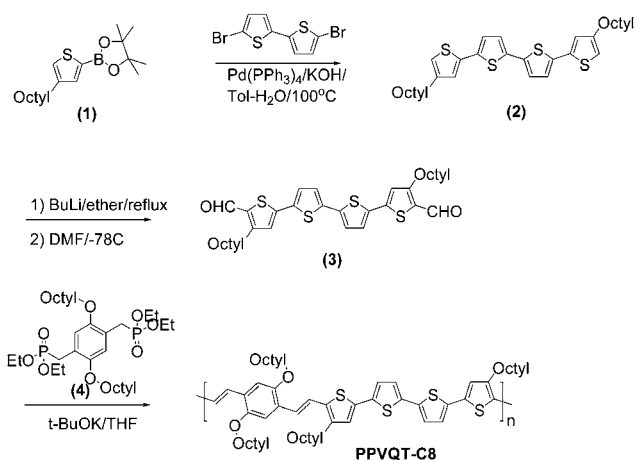
Synthesis

The structures and synthetic route to the PPVQT-C8 are shown in Scheme 1. 3-Octylthiophene was converted to a boronate (compound (1)) *via* lithiation with n-butyllithium at –78 °C, followed by treatment with 2-isopropoxy-4,4,5,5-tetramethyl-1,3,2-dioxaborolane. The 3,3-dioctylquater thiophene monomer (compound (2)) was synthesized by Suzuki coupling between compound (1) and 5,5'-dibromo-2,2'-bithiophene in toluene using Pd(PPh₃)₄ as a catalyst. Compound (2) was subsequently converted to compound (3) using BuLi. Compound (4) was

^aDepartment of Chemical Engineering, School of Environmental Science and Engineering, Pohang University of Science and Technology, Pohang, 790-784, South Korea. E-mail: kwcho@postech.ac.kr

^bDisplay Laboratory, Samsung Advanced Institute of Technology, Yongin, 446-712, South Korea

† Electronic supplementary information (ESI) available: Cyclic voltammetry data, dark-current characteristics of hole and electron only device and detailed synthetic scheme. See DOI: 10.1039/c0jm00664e



Scheme 1 Synthetic scheme for the semiconducting copolymer, PPVQT-C8, composed of quaterthiophene and phenylene vinylene units.

prepared *via* a modified previously reported method.²⁰ PPVQT-C8 was polymerized by a modified Wittig reaction between compound (3) and compound (4).

Characterization methods

^1H and ^{13}C -NMR spectra (Fig. S1–S8[†]) were measured using Bruker NMR 300 MHz (DPX 300) spectrometers. Gel permeation chromatography (GPC) analysis was performed using a PS standard column connected to a UV/refractive index detector. Cyclic voltammetry measurements were performed using a PowerLab/4SP (AD instrument) electrochemical analyzer with a glassy carbon working electrode ($d = 4$ mm), a Pt wire counter electrode, and a Ag/Ag^+ reference electrode cell in a solution of 0.1 mol L^{-1} tetrabutylammonium hexafluorophosphate (Bu_4NPF_6) in acetonitrile at a scan rate of 100 mV s^{-1} . The potential was calibrated against a ferrocene/ferrocenium couple. The energy levels were estimated using the equations: $\text{HOMO} = -(4.80 + E_{\text{onset, ox}})$, and $\text{LUMO} = -(4.80 + E_{\text{onset, red}})$.²¹

The HOMO level of the copolymer was estimated by ultraviolet photoelectron spectroscopy (AC-2, Riken Keiki Co.) UV-Visible absorption spectra were investigated using a UV-Vis spectrophotometer (Varian, CARY-5000). Grazing-incident X-ray diffraction (GI-XRD) measurements were performed using the 10C1 beamlines ($\lambda = 1.54$ Å) at the Pohang Accelerator Laboratory (PAL). The angle between the film surface and the incident beam was fixed at 0.18° . The measurements were obtained at scanning intervals of 2θ between 3° and 26° .

Solar cell device fabrication and testing

The PPVQT-C8:PCBM blend solutions were prepared in chlorobenzene at total concentrations of 10 mg mL^{-1} . After cleaning the ITO surface, PEDOT:PSS (Baytron P TP AI 4083, Bayer AG) was spin-coated to a thickness of 30 – 50 nm and baked at 120°C for 60 min. The 80 – 120 nm thick active layers were spin-coated on the PEDOT:PSS buffer layer. LiF (0.6 nm)/Al (150 nm) cathodes were formed by vacuum deposition. The J – V characteristics were measured using Keithley 4200 source/measurement units under AM 1.5 solar illumination (Oriol 1 kW

solar simulator) with respect to a reference cell PVM 132 (calibrated at the National Renewable Energy Laboratory, NREL, at an intensity of 100 mW cm^{-2}).

3. Results and discussion

The polymer possessed a molecular weight ($M_n = 20$ kDa) with a narrow size distribution (polydispersity index, $\text{PDI} = 1.57$) and was soluble in common organic solvents, such as chloroform, chlorobenzene and 1,2-dichlorobenzene. UV-Vis absorption spectra of the PPVQT-C8 and reference polymers (PQT-12 and MEH-PPV) were recorded in both solution and film states. The absorption spectrum of PPVQT-C8 in chlorobenzene solution displayed one peak at 520 nm that extended to 600 nm (Fig. 1(a)). The absorption edge was slightly red-shifted, by 50 nm, relative to the reference polymers. We speculated that the higher optical band edge of PPVQT-C8 may have been due to an internal electron donor–acceptor (D–A) interaction.²² A donor–acceptor structure can reduce the optical band gap, extending absorption down to the near infrared, and may raise the power conversion efficiency (PCE) in solar cells through increased photocurrent. In general, a low band gap polymer could result from the combination of the donor and acceptor having close HOMO level of donor and the LUMO level of acceptor.²² However, in this case, the shift of the absorption edge was relatively small, suggesting that the difference in HOMO and LUMO energy levels between *p*-divinylene phenylene and 3,3-dialkylquaterthiophene units was not significant. In the case of MEH-PPV and PPVQT-C8, the absorption edges of thin films were almost identical to those of solutions (see Fig. 1). Meanwhile, the absorption shoulder clearly appeared and the overall absorption spectra of PQT-12 films were red-shifted. This phenomenon could be interpreted

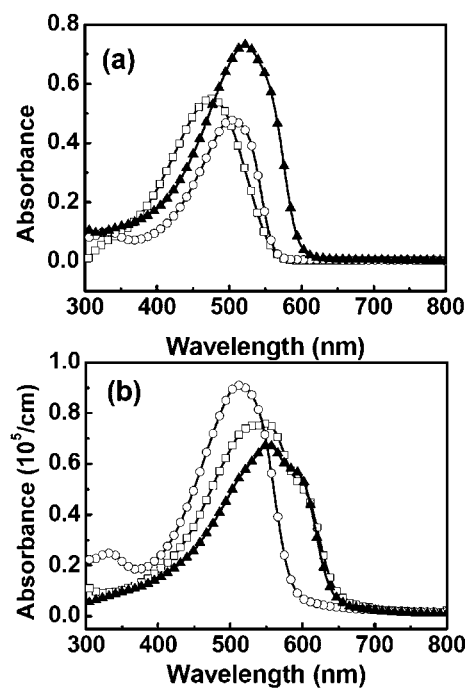


Fig. 1 UV-Vis absorption spectra of (a) solutions and (b) thin films of PPVQT-C8 and reference materials. PQT-12 (\square), MEH-PPV (\circ) and PPVQT-C8 (\blacktriangle). The film thickness was 30 ± 5 nm.

assuming that the red-shifted spectrum results from a lower energy state of delocalized excitons in the highly π -conjugated PQT-12 domains.^{23–25} As shown in Fig. 1(b), PPVQT-C8 films had a relatively high absorption coefficient compared to the reference polymers. Excellent absorption properties in p-type polymers are essential for efficient photon harvesting, which yields large photocurrents. Because the typical thickness of organic solar cells is 100–200 nm, conjugated polymers with light absorption coefficients that exceed $1 \times 10^5/\text{cm}$ in the visible and NIR regions are recommended.²⁶

The HOMO and LUMO levels of PPVQT-C8 were evaluated by cyclic voltammetry (Fig. S1†) and ultraviolet photoelectron spectroscopy (AC2 equipment). The oxidation onset ($E_{\text{onset,ox}}$) of PPVQT-C8 was found to be 0.33 V and the reduction onset ($E_{\text{onset,red}}$) was -1.52 V vs. Fc/Fc^+ . Therefore, the LUMO and HOMO levels of PPVQT-C8, estimated by cyclic voltammetry, were 5.13 and 3.28 eV, respectively, with a HOMO–LUMO gap of 1.87 eV. The HOMO level of PPVQT-C8, evaluated by ultraviolet photoelectron spectroscopy, was 5.19 eV. In the case of PQT-12, the literature values of the HOMO and LUMO levels were 5.24 and 2.97 eV.²³ Therefore, we concluded that PPVQT-C8 and PQT-12 did not differ significantly in light absorption properties and energy band structure.

Fig. 2 shows the J–V characteristics of ITO/PEDOT/PPVQT-C8:PCBM/LiF/Al devices under AM 1.5 illumination with an intensity of 100 mW cm^{-2} . The PPVQT-C8:PCBM 1 : 3 (w/w) blend device with a thickness of 100 nm showed the best performance, with a $V_{\text{oc}} = 0.67$ V, a $J_{\text{sc}} = 6.69 \text{ mA cm}^{-2}$, a $\text{FF} = 0.62$, and a $\text{PCE} = 2.8\%$. The best photovoltaic properties for devices prepared with different blend ratios and film thicknesses are listed in Table 1. With the exception of the 1 : 9 blend, the V_{oc} values of all devices were similar. Although some disagreement surrounds the origin of V_{oc} , it is widely accepted that the energy difference between the HOMO of the donor and the LUMO of the acceptor determines the V_{oc} value (0.55–0.65 V) of the P3HT:PCBM bulk heterojunction solar cell.²⁷ The HOMO level of PPVQT-C8 evaluated by CV and ultraviolet photoelectron spectroscopy was similar to that of P3HT. Therefore, the V_{oc} values for the PPVQT-C8:PCBM device could be explained by the similar HOMO levels of PPVQT-C8 and P3HT. We speculated that the V_{oc} drop for the 1 : 9 blend

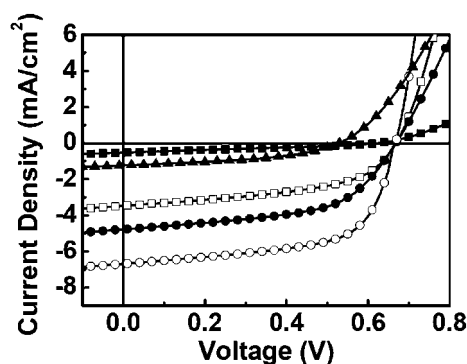


Fig. 2 J–V characteristics (AM 1.5, 100 mW cm^{-2}) of copolymer:PCBM photovoltaic (PV) cells with various blend ratios. 4 : 1 (■), 1 : 1 (□), 2 : 3 (●), 1 : 3 (○) and 1 : 9 (▲).

Table 1 Summary of the photovoltaic properties of PPVQT-C8:PCBM organic solar cell devices with various blend ratios

Blend ratio (PPVQT-C8:PCBM)	V_{oc}/V	$J_{\text{sc}}/\text{mA cm}^{-2}$	FF	PCE (%)
20% PCBM (4 : 1)	0.63	0.53	0.31	0.1
50% PCBM (1 : 1)	0.66	3.46	0.51	1.2
60% PCBM (2 : 3)	0.64	3.68	0.57	1.8
75% PCBM (1 : 3)	0.67	6.69	0.62	2.8
90% PCBM (1 : 9)	0.53	1.23	0.44	0.3

device resulted from increased direct metal-insulator-metal (MIM) contact between PCBM domains and the anode.²⁸ As shown in Fig. 3(a), the external quantum efficiency (EQE) values of the PPVQT-C8:PCBM 1 : 3 blend, in the wavelength range of 350–650 nm, were much higher than in other devices with different blend ratios. A J_{sc} of 6.69 mA cm^{-2} for the 1 : 3 blend device was reasonable because the short circuit current estimated from the EQE values²⁹ of the 1 : 3 blend device was 6.0 mA cm^{-2} . When the weight composition of PCBM exceeded 60%, the shapes of the EQE spectra resembled the absorption spectra (see Fig. 3(b)), indicating that almost all light absorption by the donor polymer contributed to the generation of photocurrent. Therefore, the 1 : 3 blend devices appeared to have well-mixed donor–acceptor interpenetrating three-dimensional (3D) networks, and the carrier mobilities appeared to be well-balanced. The low EQE and J_{sc} in the 1 : 9 blend device was likely due to the low absorption properties of the blend film. On the other hand, the relatively low J_{sc} and FF of the 4 : 1 blend device may have resulted from unoptimized bulk heterojunction morphology.

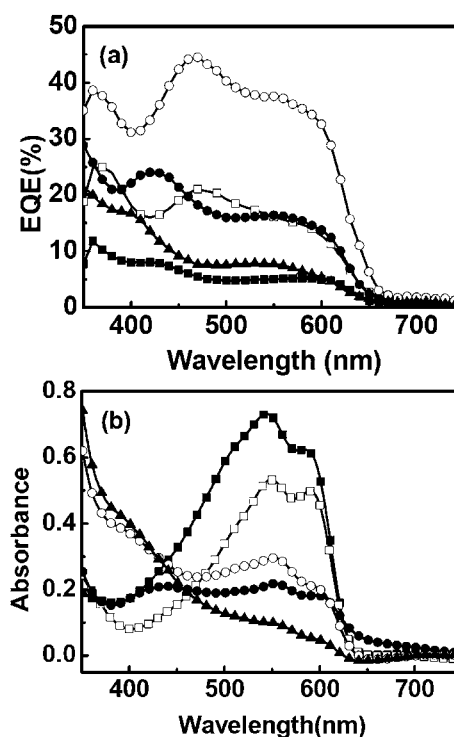


Fig. 3 (a) The EQEs and (b) UV-Vis absorption spectra of the solar cell devices with various blend ratios. 4 : 1 (■), 1 : 1 (□), 2 : 3 (●), 1 : 3 (○) and 1 : 9 (▲).

The correlation between photovoltaic performance and phase separation in the blend films was assessed by measuring the carrier mobilities (Table 2 and Fig. 4) and morphologies (Fig. 5) of PPVQT-C8:PCBM blend films. The charge-carrier mobilities of blend films were measured by means of space-charge-limited current (SCLC) measurements.^{30,31} The dark-current characteristics of ITO/PEDOT:PSS/P3HT:PCBM/Pd devices (Fig. 4(a)) were measured as a function of the bias corrected by the built-in voltage determined from the difference between the work function of the Pd and the HOMO level of PPVQT-C8. Similarly, we fabricated electron-only devices (Al/P3HT:PCBM/Al) and investigated their J–V characteristics in the dark. The SCLC mobilities were estimated using the Mott–Gurney square law,³²

$$J = (9/8)\epsilon\mu(V^2 L^{-3})$$

where ϵ is the static dielectric constant of the medium and μ is the carrier mobility. If the space charge remained in the bulk heterojunction due to low charge mobilities or to an imbalance

Table 2 Hole and electron mobilities of PPVQT-C8:PCBM films evaluated using the Mott–Gurney law ($\epsilon = 3\epsilon_0$, estimated by ellipsometry)

Blend ratio (PPVQT-C8:PCBM)	μ_h (cm ² /Vs)	μ_e (cm ² /Vs)	μ_e/μ_h
20% PCBM (4 : 1)	5.0×10^{-6}	1.0×10^{-7}	50
50% PCBM (1 : 1)	3.5×10^{-5}	1.3×10^{-4}	3.7
60% PCBM (2 : 3)	5.1×10^{-5}	1.2×10^{-4}	2.4
75% PCBM (1 : 3)	1.3×10^{-4}	3.0×10^{-4}	2.3
90% PCBM (1 : 9)	2.3×10^{-4}	6.6×10^{-4}	2.9

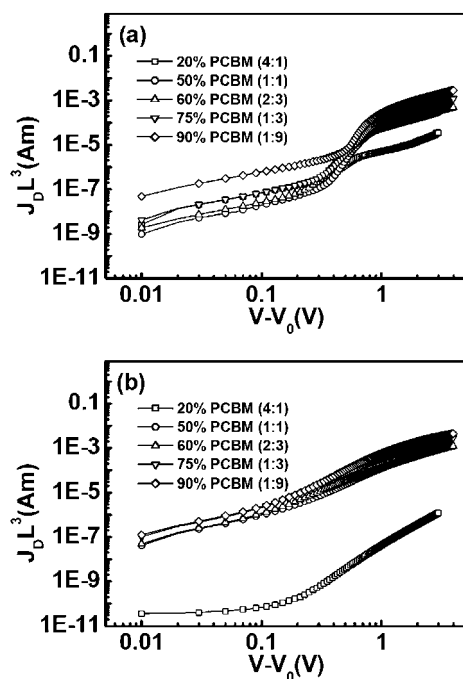


Fig. 4 Dark J–V characteristics for (a) hole-only devices (ITO/PEDOT:PSS/P3HT:PCBM/Pd) with a thickness $L = 100 \pm 10$ nm and (b) electron-only devices (Al/P3HT:PCBM/Al) with a thickness $L = 100 \pm 10$ nm.

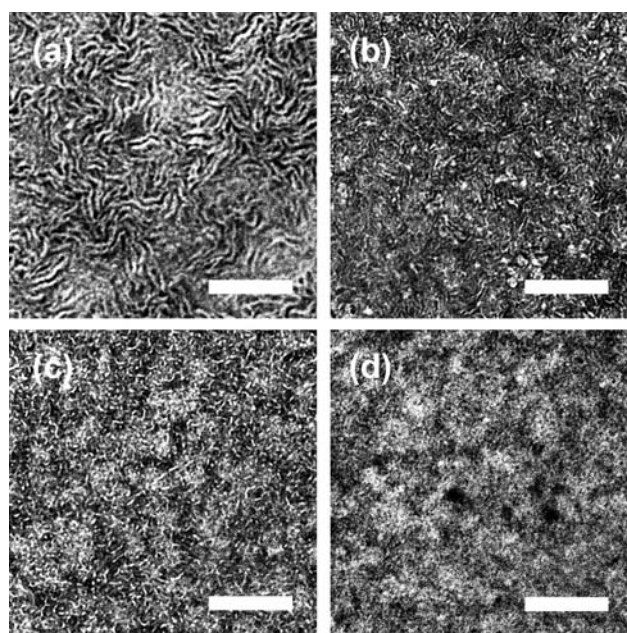


Fig. 5 Transmission electron microscopy (TEM) images of PPVQT-C8:PCBM films with various blend ratios. (a) 4 : 1, (b) 1 : 1, (c) 2 : 3 and (d) 1 : 3. The scale bar indicates 200 nm.

between the electron and hole mobilities, the photo-induced charge carriers could not be fully extracted to produce a current under the applied voltage, and the FF did not exceed 40%.^{30–34} As shown in Fig. 5(a), bright copolymer-rich lamellar domains^{35,36} developed on a length scale of 20–30 nm in 4 : 1 blend films. The presence of large lamellar copolymer domains suggested that the lack of PCBM molecules in bulk heterojunctions resulted in low electron mobility. As a result, the electron mobility of the 4 : 1 blend device extracted from the dark current was 50 times lower than the hole mobility (see Table 2). Thus, low J_{sc} and FF in the 4 : 1 blend were explained by the effects of space charge. In addition to the space charge effects, the low value of J_{sc} in the 4 : 1 blend was attributed to exciton recombination within the large copolymer domains, the size of which exceeded the typical exciton diffusion length ($L_D = 10$ nm) in semiconducting polymers. We also found that the hole mobility was lower in the 4 : 1 blend film than in the optimal blend (1 : 3). The large domains of either p-type copolymer or n-type PCBM produced dead zones for transport of the opposite carriers, and the SCLC mobility was necessarily lower than in the well-mixed case. On the other hand, the hole and electron mobilities increased up to $\sim 10^{-4}$ cm²/Vs, comparable to the SCLC mobility of P3HT,³¹ and the mobility ratio became quite small when the composition of PCBM was 60–75% (Table 2). Moreover, the PPVQT-C8 lamellar domains that induced exciton recombination disappeared if a well-mixed morphology was achieved in the 1 : 3 blend films (Fig. 5(d)). Therefore, the morphological differences indicated that the optimal composition for constructing an interpenetrating 3D network was 60–75% PCBM.

We investigated the dependence of solar cell performance on thermal treatment. Fig. 6 shows the photovoltaic parameters of thermally annealed 1 : 3 blend devices as a function of annealing temperature. Devices annealed at low temperatures (<100 °C)

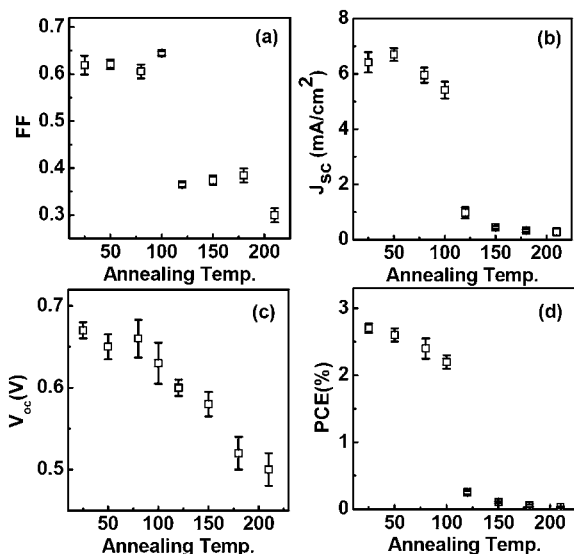


Fig. 6 The effects of thermal annealing temperature on the photovoltaic performance of the 1 : 3 blend solar cells. The annealing time was 5 min. (a) FF, (b) J_{sc} , (c) V_{oc} , and (d) power conversion efficiency.

showed insignificant changes in the photovoltaic performance. In contrast, the performances of solar cell devices based on crystalline PQT-12 or P3HT were significantly affected by thermal annealing, even at low temperatures. Solar cells based on PQT-12, underwent macrophase separation in the active layer, and the device performance dropped when the active films were annealed at high temperatures (>90 °C).^{14,15} Application of thermal annealing dramatically changed the performance of P3HT:PCBM solar cells even at low temperatures (<100 °C).^{18,19} However, annealed devices based on PPVQT-C8 yielded high efficiencies until the annealing temperature reached 120 °C. The result of this systematic thermal treatment study demonstrated that PPVQT-C8:PCBM active layers were more thermostable than a crystalline PQT-12 or P3HT case at low temperatures

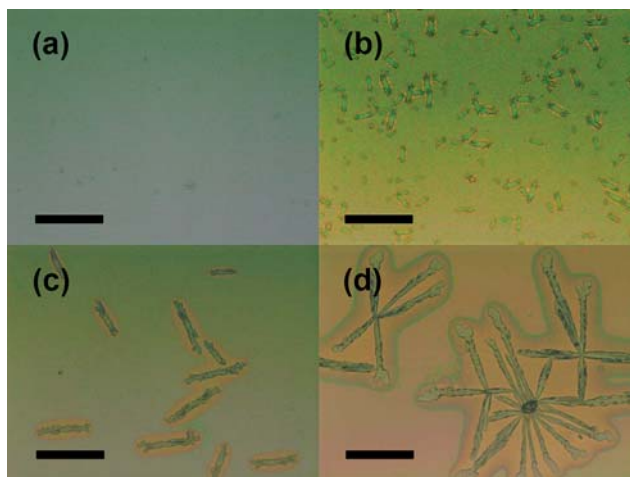


Fig. 7 Optical microscopy images of PPVQT-C8:PCBM (1 : 3) blends before and after thermal annealing at various temperatures. (a) As-prepared, (b) 120 °C, (c) 150 °C, and (d) 180 °C. The annealing time was 5 min and the scale bar indicates 50 μm .

(<100 °C). Very poor performances of thermally annealed devices at high temperatures could be attributed to the aggregation of PCBM molecules. As shown in Fig. 7, micro-domains of PCBM clusters³⁷ in films annealed above 120 °C could be observed by optical microscopy. Recent reports³⁸ that diffusion and aggregation in PCBM were faster than in crystalline P3HT at high temperatures (150 °C) lend support to this explanation. Increased exciton recombination and electron/hole mobility imbalance due to microphase separation resulted in poor values of FF and J_{sc} in devices annealed at high temperatures. Meanwhile, we confirmed that the PPVQT-C8 and PCBM molecules were stable at low annealing temperatures and maintained optimized nanoscale interpenetrating networks formed during the spin-coating process. Self-organization of the copolymer in homopolymeric and blend films during thermal annealing was investigated by GI-XRD measurements. Fig. 8(a) shows the out-of-plane diffraction patterns of as-cast and thermally annealed homopolymeric films with thicknesses of $30 \pm 5\text{nm}$. Intense (100) reflections ($2\theta = 5.1^\circ$) due to the highly oriented edge-on lamellar layer structure of PQT-12¹⁰ (d spacing, 17.3 Å) were observed after thermal annealing at 120 °C. The intensities of the (100) reflections at $2\theta = 3.4^\circ$ (d spacing, 25.9 Å) due to the lamellar

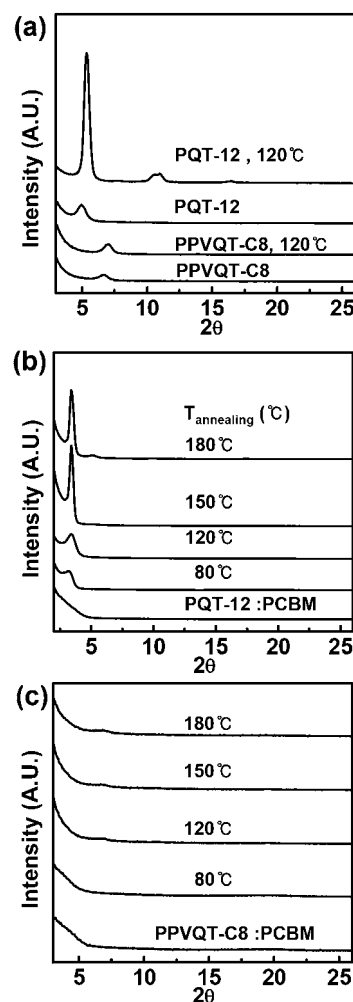


Fig. 8 Out-of-plane GI-XRD intensities for (a) PPVQT-C8 and PQT-12, (b) PQT-12:PCBM (1 : 3), and (c) PPVQT-C8:PCBM (1 : 3) films.

layer structure of the intercalated PQT-12:PCBM³⁹ dramatically increased after thermal annealing (Fig. 8(b)). However, relatively weak diffraction peaks at $2\theta = 6.6^\circ$ (d spacing, 13.4 Å) were observed in the PPVQT-C8 films, and thermal treatment induced only very small increases in the diffraction peak intensities (Fig. 8(a)). If PPVQT-C8 was mixed with PCBM in the active layer, the polymer rarely self-assembled in an edge-on orientation, even though blend films were annealed at 180 °C (Fig. 8(c)). These results support the assertion that the side chains and π - π stacking of 3,3-dialkylquaterthiophene units were significantly hindered by coupled p-divinylene phenylene units.

4. Conclusions

In conclusion, we successfully demonstrated good device performance of organic solar cells through control of the crystallinity in p-type conducting polymers. We reduced the crystallinity of PQTs without significantly changing the light absorption properties or energy band structure by introducing a p-divinylene phenylene unit between each pair of 3,3-dialkylquaterthiophene units. By optimizing the nanophase separation in the copolymer:PCBM photoactive layers, efficient photovoltaic performances with PCEs of 2.8% were obtained without further post-fabrication treatments. The highest device performances were achieved prior to PCBM aggregation at high temperatures. The present findings should assist in highly efficient organic solar cell devices with easy fabrication.

Acknowledgements

J. H. Park and J.-I. Park contributed equally to this work. This work was supported by the National Research Foundation of Korea grant (No. 2009-0093485), Manpower Development Program for Energy and Resource (MKE, 20094020100050-11-1-000) and Samsung Advanced Institute of Technology (SAIT). The authors thank the Pohang Accelerator Laboratory for providing the synchrotron radiation sources at 4C2, 8C1 and 10C1 beam lines used in this study.

References and notes

- 1 S. E. Shaheen, C. J. Brabec, N. S. Sariciftci, F. Padinger, T. Fromherz and J. C. Hummelen, *Appl. Phys. Lett.*, 2001, **78**, 841.
- 2 F. Padinger, R. S. Rittberger and N. S. Sariciftci, *Adv. Funct. Mater.*, 2003, **13**, 85.
- 3 M. Svensson, F. Zhang, S. C. Veenstra, W. J. H. Verhees, J. C. Hummelen, J. M. Kroon, O. Inganäs and M. R. Andersson, *Adv. Mater.*, 2003, **15**, 988.
- 4 M. M. Wienk, J. M. Kroon, W. J. H. Verhees, J. Knol, J. C. Hummelen, P. A. van Hal and R. A. J. Janssen, *Angew. Chem., Int. Ed.*, 2003, **42**, 3371.
- 5 F. B. Kooistra, V. D. Mihailetschi, L. M. Popescu, D. Kronholm, P. W. M. Blom and J. C. Hummelen, *Chem. Mater.*, 2006, **18**, 3068.
- 6 F. B. Kooistra, J. Knol, F. Kastenberg, L. M. Popescu, W. J. H. Verhees, J. M. Kroon and J. C. Hummelen, *Org. Lett.*, 2007, **9**, 551.

- 7 G. Dennler, M. C. Scharber and C. J. Brabec, *Adv. Funct. Mater.*, 2009, **21**, 1.
- 8 U. Zhokhavets, T. Erb, H. Hoppe, G. Gobsch and N. S. Sariciftci, *Thin Solid Films*, 2006, **496**, 679.
- 9 J. S. Kim, Y. Lee, J. H. Lee, J. H. Park, J. K. Kim and K. Cho, *Adv. Mater.*, 2010, **22**, 1355.
- 10 B. S. Ong, Y. Wu, P. Liu and S. Gardner, *J. Am. Chem. Soc.*, 2004, **126**, 3378.
- 11 D. H. Kim, Y. D. Park, Y. Jang, H. Yang, Y. H. Kim, J. I. Han, D. G. Moon, S. Park, T. Chang, C. Chang, M. Joo, C. Y. Ryu and K. Cho, *Adv. Funct. Mater.*, 2005, **15**, 77.
- 12 H. A. Becerril, N. Miyaki, M. L. Tang, R. Mondal, Y.-S. Sun, A. C. Mayer, J. E. Parmer, M. D. McGehee and Z. Bao, *J. Mater. Chem.*, 2009, **19**, 591.
- 13 M. T. Lloyd, A. C. Mayer, S. Subramanian, D. A. Mourey, D. J. Herman, A. V. Bapat, J. E. Anthony and G. G. Malliaras, *J. Am. Chem. Soc.*, 2007, **129**, 9144.
- 14 B. C. Thompson, B. J. Kim, D. F. Kavulak, K. Sivula, C. Mauldin and J. M. J. Fréchet, *Macromolecules*, 2007, **40**, 7425.
- 15 G. Wantz, F. Lefevre, M. T. Dang, D. Laliberté, P. L. Brunner and O. J. Dautel, *Sol. Energy Mater. Sol. Cells*, 2008, **92**, 558.
- 16 G. Li, Y. Yao, H. Yang, V. Shrotriya, G. Yang and Y. Yang, *Adv. Funct. Mater.*, 2007, **17**, 1636.
- 17 J. Peet, J. Y. Kim, N. E. Coates, W. L. Ma, D. Moses and A. J. Heeger, *Nat. Mater.*, 2007, **6**, 497.
- 18 W. Ma, C. Yang, X. Gong, K. Lee and A. J. Heeger, *Adv. Funct. Mater.*, 2005, **15**, 1617.
- 19 M. R. Reyes, K. Kim and D. Carroll, *Appl. Phys. Lett.*, 2005, **87**, 083506.
- 20 J. Hou, C. Yang, J. Qiao and Y. Li, *Synth. Met.*, 2005, **150**, 297.
- 21 A. J. Bard and L. A. Faulkner, *Electrochemical Methods-Fundamentals and Applications*, Wiley, New York, 1984.
- 22 E. Bundgaard and F. C. Krebs, *Sol. Energy Mater. Sol. Cells*, 2007, **91**, 954.
- 23 B. S. Ong, Y. Wu, P. Liu and S. Gardner, *Adv. Mater.*, 2005, **17**, 1141.
- 24 P. J. Brown, D. S. Thomas, A. Köhler, J. S. Wilson, J. S. Kim, C. M. Ramsdale, H. Siringhaus and R. H. Friend, *Phys. Rev. B: Condens. Matter Mater. Phys.*, 2003, **67**, 064203.
- 25 M. Sundberg, O. Inganäs, S. Stafström, G. Gustafsson and B. Sjögren, *Solid State Commun.*, 1989, **71**, 435.
- 26 K. M. Coakley and M. D. McGehee, *Chem. Mater.*, 2004, **16**, 4533.
- 27 M. C. Scharber, D. Mühlbacher, M. Koppe, P. Denk, C. Waldauf, A. J. Heeger and C. J. Brabec, *Adv. Mater.*, 2006, **18**, 789.
- 28 W. Ma, J. Y. Kim, K. Lee and A. J. Heeger, *Macromol. Rapid Commun.*, 2007, **28**, 1776.
- 29 G. Dennler, M. C. Scharber and C. J. Brabec, *Adv. Mater.*, 2006, **21**, 1.
- 30 C. Melzer, E. J. Koop, V. D. Mihailetschi and P. W. M. Blom, *Adv. Funct. Mater.*, 2004, **14**, 865.
- 31 V. D. Mihailetschi, H. Xie, B. de Boer, L. J. A. Koster and P. W. M. Blom, *Adv. Funct. Mater.*, 2006, **16**, 699.
- 32 M. A. Lampert and P. Mark, *Current Injection in Solids*, Academic Press, New York, 1970.
- 33 A. M. Goodman and A. Rose, *J. Appl. Phys.*, 1971, **42**, 2823.
- 34 V. D. Mihailetschi, J. Wildeman and P. W. M. Blom, *Phys. Rev. Lett.*, 2005, **94**, 126602.
- 35 W. Ma, C. Yang and A. J. Heeger, *Adv. Mater.*, 2007, **19**, 1387.
- 36 J. S. Moon, J. K. Lee, S. Cho, J. Byun and A. J. Heeger, *Nano Lett.*, 2009, **9**, 230.
- 37 J. S. Kim, J. H. Park, J. H. Lee, J. Jo, D.-Y. Kim and K. Cho, *Appl. Phys. Lett.*, 2007, **91**, 112111.
- 38 J. Jo, S. Kim, S. Na, B. Yu and D.-Y. Kim, *Adv. Funct. Mater.*, 2009, **19**, 866.
- 39 A. C. Mayer, M. F. Toney, S. R. Scully, J. Rivnay, C. J. Brabec, M. Scharber, M. Koppe, M. Heeney, I. McCulloch and M. D. McGehee, *Adv. Funct. Mater.*, 2009, **19**, 1173.